Photochemistry and Photobiology, 2002, 75(4): 353–361

Singlet Molecular Oxygen Quenching Ability of Carotenoids in a Reverse-micelle Membrane Mimetic System¶

Mariana A. Montenegro[1], Mónica A. Nazareno[1], Edgardo N. Durantini[2] and Claudio D. Borsarelli*[1]

[1]Instituto de Ciencias Químicas, Facultad de Agronomía y Agroindustrias, Universidad Nacional de Santiago del Estero, Santiago del Estero, Argentina and
[2]Departamento de Química y Física, Facultad de Ciencias Exactas, Fisicoquímicas y Naturales, Universidad Nacional de Río Cuarto, Río Cuarto, Argentina

Received 16 October 2001; accepted 17 January 2002

ABSTRACT

The influence of the medium heterogeneity upon the bimolecular rate constants for the physical quenching, k_q, and chemical quenching, k_r, of singlet molecular oxygen $O_2(^1\Delta_g)$ by seven natural and three synthetic carotenoids (CAR) with different substituent patterns was studied in a reverse micelle system of sodium bis(2-ethylhexyl)sulfosuccinate, hexane and water. Because $O_2(^1\Delta_g)$ was generated inside the water pools of the reverse micelles by photosensitization of the water-soluble dye rose bengal and the CAR are mainly located in the external hexane pseudophase, the quenching process was interpreted using a pseudophase model for the partition of $O_2(^1\Delta_g)$ between the water pools and the organic pseudophases. The k_q values were mainly dependent on the extent of the double-bond conjugation of the CAR, as demonstrated by a good empirical relationship between $\log(k_q)$ and the energy E(S) of the longest wavelength transition $\pi\rightarrow\pi^*$ of the CAR. In contrast, the k_r values were almost independent of the extent of the double-bond–conjugated system and about four orders of magnitude lower than k_q. However, in all cases, CAR photobleaching was observed with the formation of various oxidation products, depending on the photosensitization time. Chromatographic and spectroscopic product analysis for the reaction products of β-carotene with $O_2(^1\Delta_g)$ indicated the formation of the β-carotene-5,8-endoperoxide as the primary oxidation product.

INTRODUCTION

Carotenoid (CAR) pigments are widely distributed in nature, where they perform several biological functions. In particular, CAR play an important role in cell protection as antioxidants against free radicals and reactive oxygen species, such as singlet molecular oxygen, $O_2(^1\Delta_g)$ (1,2). In the presence of visible light the generation of $O_2(^1\Delta_g)$ in solution can be achieved *via* an energy transfer mechanism from the triplet excited state of a sensitizer molecule (S) to a ground state triplet molecular oxygen, $O_2(^3\Sigma^-_g)$(3):

$$S \xrightarrow{h\nu} {}^1S^* \xrightarrow{k_{ISC}} {}^3S^* \quad (1)$$

$${}^3S^* + O_2(^3\Sigma^-_g) \xrightarrow{k_{ET}} S + O_2(^1\Delta_g) \quad (2)$$

Hundreds of different organic, metallo-organic and inorganic compounds have been shown to be photosensitizers for biological systems (4,5). Therefore, the presence of light, air and sensitizer pigments can result in harmful effects manifested as membrane lysis, enzyme dysfunction, gene modification or cell death (or all). It has been shown that CAR act as very efficient quenchers of $O_2(^1\Delta_g)$, competing with the unimolecular decay pathway (Eq. 3) *via* both physical (energy transfer) (Eq. 4) (6) and chemical processes (Eq. 5) (7).

$$O_2(^1\Delta_g) \xrightarrow{k_d} O_2(^3\Sigma^-_g) \quad (3)$$

$$O_2(^1\Delta_g) + CAR \xrightarrow{k_q} O_2(^3\Sigma^-_g) + {}^3CAR^* \quad (4)$$

$$O_2(^1\Delta_g) + CAR \xrightarrow{k_r} CARO_2 \quad (5)$$

Thus, CAR protect biological targets from $O_2(^1\Delta_g)$ damage. This protective function by CAR is highly efficient because the chemical quenching rate constant k_r is several orders of magnitude lower than the physical quenching rate constant k_q (4). Once produced, the triplet excited state of the CAR ^{3}CAR* can return to the ground state dissipating the energy excess as heat. Thus, the CAR acts as a catalyst in the de-

Dedicated to Professor Silvia E. Braslavsky on the occasion of her 60th birthday.

¶Posted on the website on January 28, 2002.

*To whom correspondence should be addressed at: Instituto de Ciencias Químicas, Facultad de Agronomía y Agroindustrias, Universidad Nacional de Santiago del Estero, Av. Belgrano (S) 1912, 4200 Santiago del Estero, Argentina. Fax: 54-385-4509585; e-mail: cborsa@unse.edu.ar

Abbreviations: AOT, sodium bis(2-ethylhexyl)sulfosuccinate; CAR, carotenoid; CC, open-column chromatography; DMA, 9,10-dimethylanthracene; DMF, dimethylformamide; DMSO, dimethylsulfoxide; HPLC, high-performance liquid chromatography; $O_2(^1\Delta_g)$, singlet molecular oxygen; RB, rose bengal; S, sensitizer molecule; TLC, thin-layer chomatography; TRPD, time-resolved phosphorescence detection; UV–Vis, UV–visible spectroscopy; *W*, water to AOT molar ratio.

activation of $O_2(^1\Delta_g)$. Over the last few years, $O_2(^1\Delta_g)$ quenching by CAR has received considerable attention in homogeneous media (8–16), as opposed to organized media (17–19).

Because of the complexity of biological media, where compartmentalization effects play an important role in chemical reactivity, the study of chemical and photochemical processes in microheterogeneous media is of current interest; the aim is to simulate the heterogeneity present in biological systems (20,21). The reactivity of $O_2(^1\Delta_g)$ toward several substrates in the organized media has been reviewed by Lissi *et al.* (22). Among microheterogeneous systems reverse micelle is a useful and simple model of biological systems. They present three different sites where the substrates can be located: an internal aqueous microphase (water pool), the interface region containing the monolayer of surfactant molecules and the external organic phase (23). These systems have been used as models for $O_2(^1\Delta_g)$-mediated photo-oxidations of 1,3-diphenylisobenzofuran (24), amino acids (25–28), anthracene (29) and phenolic derivatives (30).

To our knowledge, no information is available on the reactivity of CAR toward $O_2(^1\Delta_g)$ in reverse micelle systems. The aim of this work is to examine the quenching (physical + chemical) processes of $O_2(^1\Delta_g)$ by a series of naturally occurring and artificial CAR with different substituent patterns in reverse micelles made with the surfactant sodium bis(2-ethylhexyl)sulfosuccinate (AOT), *n*-hexane and water using the water-soluble dye rose bengal (RB) as the photosensitizer. The chemical structure of natural and synthetic CAR used in this work is shown in Fig. 1.

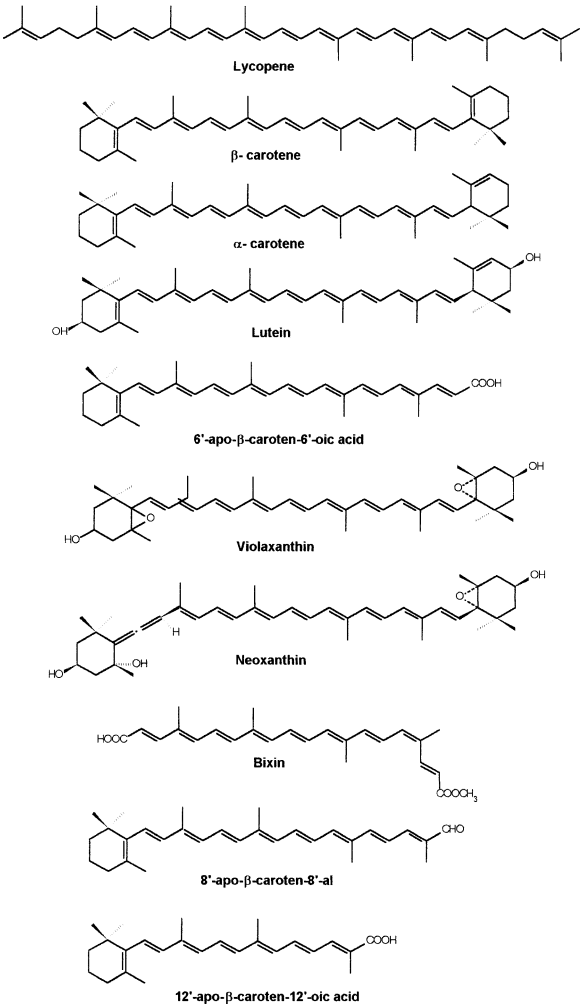

Figure 1. The chemical structure of natural and synthetic CAR used in this work.

EXPERIMENTAL SECTION

Materials. The sodium salt RB from Sigma Chemical Co. (St. Louis, MO), 9,10-dimethylanthracene (DMA) (99%) from Aldrich (Milwaukee, WI) and sodium hydroxide from Meck Química Argentina SAIC (Buenos Aires, Argentina) were used as received. AOT (Sigma) was dried under vacuum and used without further purification. Hexane (HPLC grade) from Sintorgan S.R.L. (Buenos Aires, Argentina) was used as received. Water was triply distilled.

Carotenoids. Natural CAR pigments were extracted, isolated and purified from natural sources. The extraction and purification procedures were performed under reduced light conditions, and the purified CAR were stored under nitrogen atmosphere at −20°C to avoid further decomposition (31). The methodologies for the extraction and purification of naturally occurring CAR have been described elsewhere (32–34). In summary, the pigments were extracted out with cold acetone, and the pigment extract was transferred to petroleum ether and washed with water. In some cases, saponification of the extract was necessary to hydrolyze the esters or remove the chlorophylls. This alkaline hydrolysis was performed with 10% potassium hydroxide in methanol for 12 h at room temperature and in the dark. The alkali was removed by washing with water several times, and the solvent was removed under reduced pressure. The purification procedure was done by open-column chromatography (CC) on magnesium oxide–hyflosupercel mixture (1:2) eluted with petroleum ether and increasing amounts of ethyl ether or acetone. Subsequent rechromatography of the fractions was performed on silica gel plates or by CC. Identification and quantitative analysis of the pigments were performed by thin-layer chromatography (TLC), high-performance liquid chromatography (HPLC) and UV–visible spectroscopy (UV–Vis) (35,36). The purity of the samples obtained was greater than 95%. The CAR obtained by this method were α-carotene (β,ε-carotene), from carrot or squash (*Cucurbita moschata*); β-carotene (β,β-carotene); lutein (β,ε-carotene-3,3′-diol); violaxanthin (5,6,5′,6′-diepoxy-5,6,5′,6′-tetrahydro-β,β-carotene-3,3′-diol) and neoxanthin (5,6-epoxy-6,7-didehydro-5,6,5′,6′-tetrahydro-β,β-carotene-3,5,3′-triol), from Swiss chard (*Beta vulgaris* var. cycla) and lycopene (ψ,ψ-carotene), from tomato (*Lycopersicum esculentum*). Bixin (methyl hydrogen 9′*Z*-6,6′-diapocarotene-6,6′-dioate) was extracted from *Bixa orellana* L. seeds by successive extractions with petroleum ether and a (1:1) mixture of methanol and dichloromethane. The extracts were filtered and concentrated under reduced pressure conditions. Purification was carried out by preparative TLC on silica gel plates eluted with ethyl acetate–petroleum ether (3:2), removing the upper fraction and repeating this process twice.

Synthesis of the CAR. 12′-Apo-β-caroten-12′-oic and 6′-apo-β-caroten-6′-oic acids were synthesized as previously reported (37,38), starting from retinal (Sigma) and 8′-apo-β-caroten-8′-al (Hoffman-La Roche, Basel, Switzerland). All products showed the corresponding characteristic spectra reported earlier (38).

Preparation of reverse micelle solutions. A stock solution of 0.1 *M* AOT was prepared in *n*-hexane. Subsequently, 5 μL of an aqueous stock solution of RB was added with a microsyringe to 2 mL of the AOT solution placed in a quartz cuvette (1 cm optical path). The final dye concentration was *ca* 5 μ*M*. Additional water was added with a microsyringe. The total amount of water present in the system was expressed as the molar ratio between water and the surfactant ($W = [H_2O]/[AOT]$) and varied between 5 and 50. The mixtures were mildly shaken to obtain optically transparent solutions. CAR or the actinometer DMA (or both) were incorporated by injecting *ca* 50 μL from appropriated stock solutions in *n*-hexane.

Instrumentation. HPLC experiments were performed on a Konik 500A liquid chromatograph equipped with a C_{18} Vydac 218TP54 (5 μm, 4.6 × 250 mm) or a C_{18} Spherisorb ODS-2 (5 μm, 4.6 × 250

Table 1 UV–Vis absorption and fluorescence properties of the sensitizer rose bengal (RB) in homogeneous and in 0.1 *M* AOT/hexane/water reverse micelle solutions as a function of *W* (=[H_2O]/[AOT]).

Solvent	λ_{abs} (nm)	λ_f (nm)	Φ_f*	τ_f (ps)†
AOT *W* = 1	559	575	0.092	930
AOT *W* = 2	559	575	0.063	710
AOT *W* = 5	559	575	0.040	420
AOT *W* = 10	559	575	0.035	310
AOT *W* = 50	559	575	0.029	250
Methanol	558‡	573	0.080‡	476
Ethanol	557‡	566	0.110‡	—
Water	549§	567	0.010‡	80

*±5%.
†0.25 *M* AOT–isooctane (Rodgers [40]).
‡Neckers (39).
§Green (44).

mm) column and a Konik UV–Vis 200 detector operating at 450 nm.

Stationary photolysis experiments were performed with a 150 W filament lamp coupled with an orange cut off filter ($\lambda > 530$ nm). UV–Vis spectra were recorded with an HP 8453 diode-array spectrophotometer. Steady-state fluorescence spectra of RB were measured with a Hitachi F-2500 spectrofluorometer in air-equilibrated RB solutions with absorbances matched within 5% at 520 nm (the excitation wavelength). Fluorescence quantum yields, Φ_f, were calculated using the RB fluorescence in water ($\Phi_f = 0.01$) (39) as a standard. In all cases, the quantum yields were corrected for the difference in refractive index of the media.

$O_2(^1\Delta_g)$ sensitization was measured using a time-resolved phosphorescence detection method (TRPD). A Q-switched Nd:YAG laser (Spectron SL400) operating at the frequency-doubled output (532 nm, 20 ns halfwith) was used to excite the sensitizer RB. The $O_2(^1\Delta_g)$ phosphorescence (mainly 1270 nm) was detected at right angles with a Judson J16/8Sp germanium photodiode detector, after passing through appropriate filters. The output of the detector was fed *via* amplifier stages to a Hewlett–Packard HP-54504A digital oscilloscope and then to an on-line PC. About 20 cycles were usually needed for averaging the decay times to obtain a good signal-to-noise ratio.

All experiments were performed in duplicate in air-equilibrated solutions and under controlled temperature of 25 ± 1°C.

RESULTS AND DISCUSSION

Localization of RB and CAR in AOT reverse micelles

Table 1 summarizes some photophysical parameters of RB in reverse micelles and homogeneous media. As compared with water, the position of the UV–Vis and fluorescence maxima of RB in reverse micelle media is redshifted by *ca* 10 nm, independent of the *W*(=[H_2O]/[AOT]) value.

In addition, the fluorescence quantum yield of the dye decreases with *W* and was correlated with the fluorescence lifetime of RB, as determined in a similar AOT reverse micelle system (40) (Table 1). Because RB is an anionic dye insoluble in nonpolar organic solvents, one should expect its location to be in the water pool of the reverse micelle system. However, the above results indicate that even at large *W* values in the reverse micelle solution, RB senses an environment similar to methanol rather than water. This photophysical behavior of RB can be explained in terms of the changes produced in the properties of the water pool and the water–surfactant interface as the amount of water is increased (41–43). At low *W* values (*i.e.* $W < 5$) the water molecules in the micellar core can be assumed to be strongly associated or bound to the micellar interface, solvating the polar head groups and the sodium counterions of AOT (41). Thus, RB senses a highly structured environment with a larger local viscosity, increasing both fluorescence quantum yield and lifetime. As *W* increases, the local viscosity in the micellar core and in the micellar interface is strongly reduced, and the proportion of free water molecules at the micellar core increases until the water environment resembles that of bulk water (41,43). However, at $W = 50$ the photophysical properties of RB in reverse micelles do not correspond to those for bulk water, indicating that the dye remains associated with the water–surfactant interface, which is somewhat less polar than the water core region (42). Despite its anionic nature RB remains associated with the water–surfactant interface because of the effect of hydrophobic forces; this is because its solubility in homogeneous ethanol is almost three times greater than that in water (44).

In reverse micellar systems nonpolar compounds are expected to be mainly located in the external organic phase. This should be the case for the carotenes (C_xH_y-CAR–type compounds), such as lycopene, α- and β-carotene. The fine spectral structure of CAR has shown that the ratio of the peak height %III/II is a useful parameter of their functional group or environmental characterization (or both) (36,45). The ratio %III/II was calculated by taking as the baseline or zero value the valley between the longest wavelength absorption band (designated as III) and the middle absorption band (usually λ_{max}; designated as II). For CAR without the spectral vibration structure, the ratio %III/II is considered to be zero (36). As can be seen in Table 2, the absorption maxima position and the %III/II ratio in AOT media for the carotenes were almost the same as those observed in hexane.

However, in AOT media the UV–Vis spectra of xanthophylls ($C_xH_yO_z$-CAR–type compounds) were dependent on the composition of the reverse micelle solution (Table 2). As *W* increases, CAR, such as lutein, violaxanthin and bixin, showed a small redshift of the absorption bands and a reduction of the ratio %III/II, with similar values observed in ethanol. Nevertheless, the spectral features in AOT reverse micelle solutions were completely different, compared with those observed in water and in EtOH:H_2O mixtures (Table 2). These results indicate that in AOT media the xanthophylls interact with the micellar interface.

Recently, Correa *et al.* (38) have reported the binding of the synthesized CAR series 6′-apo-β-caroten-6′-ol, 6′-apo-β-caroten-6′-oic acid and ethyl 6′-apo-β-caroten-6′-oate to the AOT interface. For the ester derivative no significant binding was observed. They calculated the values for the binding constant, K_b, which were 3 and 320 M^{-1} for the alcohol and the acid derivatives at $W = 0$ and 10, respectively, as measured by absorbance changes as a function of the surfactant concentration. They claimed that the driving force for the binding to the AOT interface is given by the ability of CAR with –OH or –COOH end groups to interact specifically with the polar heads of AOT by hydrogen bonding, independent of the presence of water (38). By assuming a similar binding behavior for the natural xanthophylls, the above K_b values imply that the percentage of CAR bound to the micellar interface in 0.1 *M* AOT reverse micelle solu-

Table 2 UV–Vis absorption maxima of the band II and III of carotenoids and its respective %III/II ratio in homogeneous and in 0.1 *M* AOT–hexane–water reverse micelle solutions as a function of *W* (=[H_2O]/[AOT]).

Carotenoid	Solvent	λ_{max} (nm)* band II	λ_{max} (nm)* band III	%III/II ratio
β-Carotene	Ethanol	452	476	27 ± 1
	Hexane	451	479	39 ± 2
	EtOH: H_2O (50:50 vol/vol)	458	486	32 ± 2
	AOT *W* = 5	451	479	39 ± 2
	AOT *W* = 20	451	479	38 ± 2
Lycopene	Ethanol	473	504	62 ± 2
	Hexane	472	502	81 ± 2
	EtOH: H_2O (90:10 vol/vol)	472	503	36 ± 2
	AOT *W* = 5	473	502	78 ± 2
	AOT *W* = 30	472	503	79 ± 2
Lutein	Ethanol	446	474	63 ± 2
	Hexane	444	473	68 ± 2
	EtOH: H_2O (50:50 vol/vol)†	447	473	40 ± 2
	AOT *W* = 5	446	475	63 ± 2
	AOT *W* = 30	446	475	61 ± 2
Violaxanthin	Ethanol	440	470	95 ± 2
	Hexane	440	465	98 ± 2
	AOT *W* = 5	444	474	96 ± 2
	AOT *W* = 30	444	474	94 ± 2
Bixin	Ethanol	456	483	27 ± 1
	Hexane	455	486	63 ± 2
	EtOH: H_2O (50:50 vol/vol)	457	485	3 ± 1
	Water‡	443	–	0
	AOT *W* = 5	457	488	56 ± 2
	AOT *W* = 30	457	488	47 ± 2

*±1 nm.
†A new band appears at 370 nm.
‡The spectral fine structure is lost.

tions is *ca* 95 and 25% for the carboxylic and alcohol CAR derivatives, respectively.

Therefore, it can be assumed that the CAR bound to the AOT reverse micelles are forming a part of the micellar interface, with their polar groups interacting with the surfactant polar heads and their hydrophobic-conjugated double-bound moiety oriented toward the nonpolar hexane pseudophase.

Singlet oxygen production and quenching rate constants by CAR in AOT reverse micelles

The results shown previously indicate that the micellar interface separates the site of location of the sensitizer from that of the CAR. Taking into account the AOT concentration used in this work and the surfactant aggregation numbers of the AOT–hexane system at different *W* values (46), the concentration of reverse micelle aggregates is at least two orders of magnitude larger than those of the sensitizer and the CAR. Assuming a Poisson distribution for the solutes in the micellar system, this means that less than 5% of the micellar aggregates are occupied by a single RB or a bound CAR molecule. Furthermore, the probability to localize both a sensitizer and a CAR molecule in the same micellar aggregate is much lower (<0.25%).

Because the sensitizer RB is located in the water–surfactant interface, the reactive species $O_2(^1\Delta_g)$ is generated inside the reverse micelle (Eqs. 1 and 2); therefore, this species must diffuse to the nonpolar pseudophase (*i.e.* the external side of the micellar interface or the hexane pseudophase [or both]) in order to interact with the CAR. It has been reported that the decay kinetic behavior of $O_2(^1\Delta_g)$ in microheterogeneous systems is affected by its distribution equilibrium between hydrophilic and hydrophobic pseudophases (22). Lee and Rodgers (47) have proposed a kinetic model for the distribution equilibrium and decay of $O_2(^1\Delta_g)$ and for its quenching by water-soluble quenchers in micellar dispersions (25). We assumed the same kinetic model for the decay of $O_2(^1\Delta_g)$ in the presence of CAR in a reverse micelle solution, which is represented in Fig. 2.

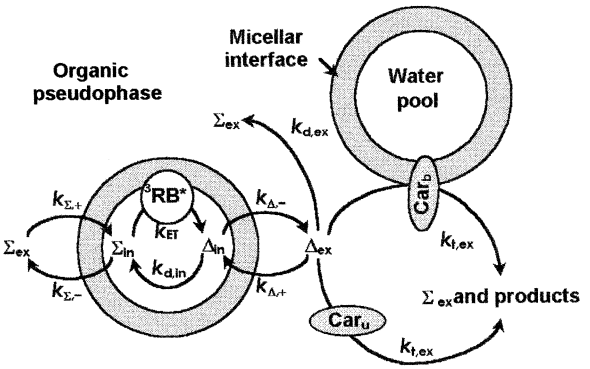

Figure 2. Schematic representation of the location of RB and CAR, the pseudophase model for the equilibrium distribution of molecular oxygen species and quenching of $O_2(^1\Delta_g)$ by CAR in AOT reverse micelle solutions.

In Fig. 2 ^{3}RB* represents the excited triplet state produced upon light excitation of the dye; Σ_{ex}, Σ_{in} and Δ_{ex}, Δ_{in} are the $O_2(^3\Sigma^-_g)$ and $O_2(^1\Delta_g)$ concentrations in the interior (water pool) and exterior (organic solvent + micellar interface) pseudophases, respectively. In turn, $k_{\Sigma,+}$, $k_{\Sigma,-}$ and $k_{\Delta,+}$, $k_{\Delta,-}$ define the unimolecular entrance and exit rate constants for both molecular oxygen species; $k_{d,in}$ and $k_{d,ex}$ are the decay rate constants for $O_2(^1\Delta_g)$ in both pseudophases, and $k_{t,ex}$ is the total bimolecular quenching rate constant of $O_2(^1\Delta_g)$ by the CAR in the organic pseudophase. CAR_u and CAR_b represent the unbound and bound CAR to the micellar interface, respectively. As was discussed previously (47), the kinetic analysis of this pseudophase model is simplified if it is assumed that both $O_2(^3\Sigma^-_g)$ and $O_2(^1\Delta_g)$ equilibration between the internal and external pseudophases are much more rapid in comparison with the rate of $O_2(^1\Delta_g)$ decay in both pseudophases, *i.e.* if $k_{\Sigma,+}$, $k_{\Sigma,-}$ and $k_{\Delta,+}$, $k_{\Delta,-} \gg k_{d,in}$, $k_{d,ex}$. This condition is fulfilled because the $k_{\Sigma,+}$ and $k_{\Sigma,-}$ values (and those for $k_{\Delta,+}$ and $k_{\Delta,-}$) have been reported to be not less than 1×10^7 s^{-1} in micellar media (48), which are at least two orders of magnitude larger than the decay of $O_2(^1\Delta_g)$ in aqueous or in hydrocarbon media (4). Under this condition, it is expected that both Δ_{ex} and Δ_{in} species decay with a common lifetime, *i.e.* $\tau_\Delta = 1/k_d$, (47,49). As a consequence of the fast equilibration condition, the equilibrium constant of $O_2(^1\Delta_g)$ between the two pseudophases is given by Eq. 6:

$$K_\Delta = \frac{[\Delta_{in}]}{[\Delta_{ex}]} = \frac{k_{\Delta,+}}{k_{\Delta,-}} \qquad (6)$$

where $[\Delta_{in}]$ and $[\Delta_{ex}]$ are the corresponding $O_2(^1\Delta_g)$ concentrations in the internal and external pseudophases, respectively. In accordance with the pseudophase model (47) the decay of $O_2(^1\Delta_g)$ in both pseudophases is given by Eq. 7:

$$\frac{d[\Delta_T]}{dt} = f\frac{d[\Delta_{in}]}{dt} + (1 - f)\frac{d[\Delta_{ex}]}{dt} \quad (7)$$

where f and $(1 - f)$ are the weighing coefficients equal to the volume fractions of the interior and exterior compartments, and $[\Delta_T]$ refers to the total $O_2(^1\Delta_g)$ concentration. In our case Eq. 7 can be rewritten taking into account the fact that the quenching process occurs in the external pseudophase with a total quenching (physical + chemical) rate constant $k_{t,ex} = k_{q,ex} + k_{r,ex}$:

$$-\frac{d[\Delta_T]}{dt} = fk_{d,in}[\Delta_{in}] + (1 - f)(k_{d,ex}[\Delta_{ex}] + k_{t,ex}[\Delta_{ex}][Car]_{ex}) \quad (8)$$

Here $[Car_{ex}]$ represents the total CAR concentration in the external pseudophase that includes the bound and unbound CAR because the double-bond–conjugated system of the bounded CAR is located in the nonpolar region of the micellar interface. Because both Δ_{in} and Δ_{ex} decay with a common lifetime $\tau = 1/k_d$ (*vide supra*), the decay of $O_2(^1\Delta_g)$ can also be written as:

$$-\frac{d[\Delta_T]}{dt} = k_d[\Delta_T] = k_d(f[\Delta_{in}] + (1 - f)[\Delta_{ex}]) \quad (9)$$

Finally, combining Eqs. 6, 8 and 9 and considering that the bulk CAR concentration $[Car_T] = (1 - f)[Car_{ex}]$, Eq.10 is obtained:

$$k_d = \frac{fk_{d,in}K_\Delta + (1 - f)k_{d,ex}}{fK_\Delta + (1 - f)} + \frac{k_{t,ex}}{fK_\Delta + (1 - f)}[Car_T] = k_{d,o} + k_{t,ap}[Car_T] \quad (10)$$

where $k_{d,o}$ $(= \tau_o^{-1})$ is the decay rate constant of $O_2(^1\Delta_g)$ in the absence of CAR, and $k_{t,ap}$ is the apparent total quenching rate constant. Both $k_{d,o}$ and $k_{t,ap}$ are functions of the volume fraction of dispersed pseudophase, f, and of the equilibrium constant of $O_2(^1\Delta_g)$ between both pseudophases, K_Δ. For our calculations we use $K_\Delta = 0.11$, as measured by Lee and Rodgers in AOT–heptane and AOT–isooctane reverse micelles (47), assuming similar solubility and diffusion properties of molecular oxygen in AOT–hexane systems. The volume fraction f depends on the amount of water and surfactant present in the solution and was calculated using 389 cm^3/mol as the molar volume of AOT (46). Thus, in 0.1 M AOT reverse micelle solutions the values of f vary between 0.048 and 0.129 at $W = 5$ and 50, respectively.

Figure 3 shows typical $O_2(^1\Delta_g)$ phosphorescence signals observed at 1270 nm upon laser pulsed excitation at 532 nm of RB in air-equilibrated AOT reverse micelle solutions in the absence and presence of β-carotene. Under our experimental conditions the rate of formation of $O_2(^1\Delta_g)$ (which is given by the rate of the energy-transfer quenching process of ^{3}RB by $O_2(^1\Delta_g)$, Eq. 2) is much faster than its rate of decay and the instrumental response risetime (<7 μs, in our experimental set up). The decay portion of the signals after 10 μs of the laser pulse showed an exponential behavior in agreement with the $O_2(^1\Delta_g)$ fast equilibrium assumption of the pseudophase model (see previously) and were fitted with a first-order decay law (50).

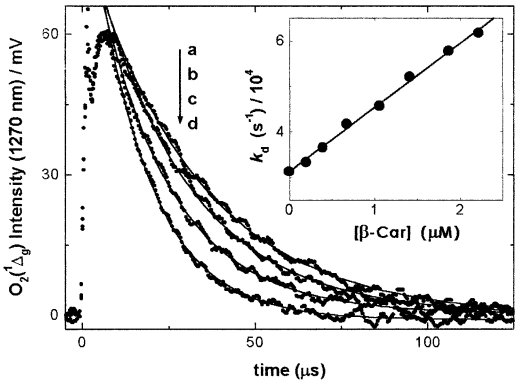

Figure 3. Signals of the $O_2(^1\Delta_g)$ phosphorescence detected at 1270 nm in 0.1 M AOT–hexane–water ($W = 5$) reverse micelle solution at several β-carotene concentrations: (1) 0.0 μM; (2) 0.4 μM; (3) 1.1 μM; and (4) 2.2 μM. Solid lines represent the monoexponential fitting of the signals. Inset: Stern–Volmer quenching plot.

$$I_t = I_o\exp(-t/\tau) \quad (11)$$

where $\tau = k_d^{-1}$ is the $O_2(^1\Delta_g)$ lifetime, and I_o refers to the amplitude of the signal at ''zero'' time, which is proportional to the quantum yield of $O_2(^1\Delta_g)$ production, Φ_Δ (50). Redmond (51) has reported $\Phi_\Delta = 0.8$ for RB in AOT reverse micelle systems, which is close to that observed in homogeneous solvents (5). Under the same experimental conditions we did not observe significant difference in the I_o values observed between $5 \leq W \leq 50$, indicating that Φ_Δ remains almost constant or that the quencher does not consume the sensitizer (or both). In the absence of the quencher, the $O_2(^1\Delta_g)$ lifetime (k_o^{-1}) in reverse micelles was dependent on f, in accordance with Eq. 10, with values ranging between 32.5 and 30.2 μs at $W = 5$ and 50, respectively. Assuming that the $O_2(^1\Delta_g)$ diffusion coefficient in the AOT–hexane system is similar to that in hexane (50), apparently the $O_2(^1\Delta_g)$ travels *ca* 600 nm, crossing several reverse micelle aggregates during its lifetime.

In all cases, plots of k_d *vs* $[Car_T]$ (Eq. 10) were linear, yielding $k_{t,ap}$ from the slopes values, as is shown in the inset of Fig. 3. Table 3 shows the respective values of $k_{t,ex}$ obtained with Eq. 10. As mentioned previously, $k_{t,ex}$ includes the physical and the chemical quenching pathways of $O_2(^1\Delta_g)$ by the CAR. In order to evaluate the reactive quenching rate constant, $k_{r,ex}$, we use DMA as the reference compound, which is expected to be located in the external pseudophase (29). Under steady-state irradiation the rate of consumption of a substrate P located in the external pseudophase (such as DMA and the CAR) is given by:

$$-\frac{d[P]}{dt} = (1 - f)k_{r,ex}[\Delta_{ex}][P_{ex}] = k_{r,ex}[\Delta_{ex}][P_T] = k_{r,ap}[P_T] \quad (12)$$

According to this rate law the photo-oxidation process of both DMA and the CAR should follow a first-order kinetics decay, as is shown in the inset of Fig. 4. The bimolecular rate constant for the photooxidation of DMA in AOT–hex-

Table 3 Bimolecular rate constants for the total ($k_{t,ex}$) and reactive ($k_{r,ex}$) quenching of $O_2(^1\Delta_g)$ by carotenoids in 0.1 *M* AOT/hexane/water reverse micelle as a function of *W* (=[H_2O]/[AOT]) and energy *E*(*S*) of the longest wavelength transition $\pi \rightarrow \pi^*$ ($1^1A_g \rightarrow 1^1B_u$).

Carotenoid	*W*	$k_{t,ex}/10^{10}$ (M^{-1} s^{-1})	$k_{r,ex}/10^{6}$ (M^{-1} s^{-1})	*E*(S) ($\times 10^3$ cm^{-1})
Lycopene (1)	5	2.0 ± 0.1	2.1 ± 0.2	19.92
	10	2.2 ± 0.1	2.1 ± 0.2	
	20	2.6 ± 0.2	2.0 ± 0.2	
	50	2.5 ± 0.1	2.3 ± 0.2	
β-Carotene (2)	5	1.3 ± 0.1	1.1 ± 0.1	20.92
	20	1.2 ± 0.1	0.8 ± 0.1	
	50	1.3 ± 0.1	0.9 ± 0.1	
α-Carotene (3)	5	1.3 ± 0.1	1.6 ± 0.1	21.14
	20	1.2 ± 0.1	1.7 ± 0.1	
	50	1.3 ± 0.1	1.6 ± 0.1	
Lutein (4)	5	1.2 ± 0.2	1.8 ± 0.4	21.05
	20	1.0 ± 0.1	1.6 ± 0.3	
	50	0.9 ± 0.1	1.8 ± 0.5	
6′-apo-β-caroten-6′-oic acid (5)	5	1.0 ± 0.1	1.4 ± 0.1	20.79
	20	1.0 ± 0.1	1.7 ± 0.5	
	50	0.9 ± 0.1	2.1 ± 0.5	
Violaxanthin (6)	5	1.0 ± 0.1	1.0 ± 0.1	21.23
	50	0.8 ± 0.1	0.8 ± 0.1	
Neoxanthin (7)	5	0.9 ± 0.1	1.8 ± 0.1	21.41
	50	0.9 ± 0.1	1.8 ± 0.2	
Bixin (8)	5	1.6 ± 0.1	1.6 ± 0.1	20.49
	50	1.0 ± 0.1	1.7 ± 0.3	
8′-apo-β-caroten-8′-al (9)	5	1.1 ± 0.1	1.1 ± 0.1	20.88
	20	1.1 ± 0.1		
	50	1.1 ± 0.1	1.2 ± 0.1	
12′-apo-β-caroten-12′-oic acid (10)	5	0.04 ± 0.02	1.9 ± 0.2	22.37*
	20	0.04 ± 0.02	2.0 ± 0.6	
	50	0.03 ± 0.01	2.4 ± 0.8	

*Band threshold.

ane reverse micelles, $k_{r,ex}^{DMA}$, was obtained using the TRPD method (Eq. 10) because the $O_2(^1\Delta_g)$ quenching process by this compound goes exclusively through a chemical reaction (29). A $k_{r,ex}^{DMA} = 9 \times 10^6$ M^{-1} s^{-1} value was obtained independent of *W*, as expected for a compound located exclusively in the external pseudophase (29,30). Thus, the $k_{r,ex}$ values (Table 3) for the CAR were calculated by a comparison of the $k_{r,ap}$ values obtained for the CAR and DMA under identical experimental condition.

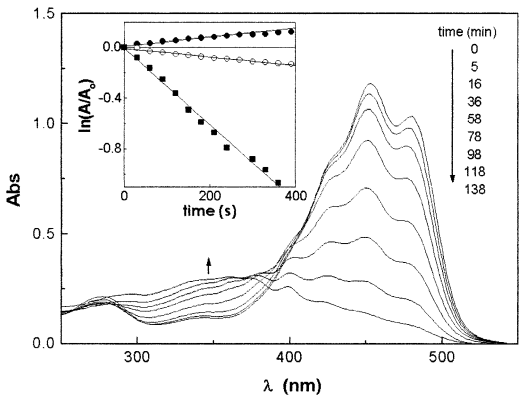

Figure 4. UV–Vis absorption changes produced in 0.1 *M* AOT–hexane–water (*W* = 5) reverse micelle solution containing 1 μ*M* β-carotene and 5 μ*M* RB, observed upon excitation at the absorption band of the sensitizer RB (λ > 530 nm). Inset: first-order kinetic plots for the consumption of β-carotene (<5% of conversion of the CAR) monitored at (●) 375 nm and (○) 500 nm and for the actinometer DMA monitored at 398 nm (■).

CAR bleaching involving superoxide anion, $O_2^{\bullet -}$, generated by RB photosensitization is disregarded because it has been shown that in an aqueous solution or a biological environment this is a very inefficient process (52). Furthermore, no CAR bleaching was detected in a N_2-saturated solution, discarding reaction pathway from the excited triplet state of RB.

From the data shown in Table 3, it is observed that $k_{t,ex} \gg k_{r,ex}$; therefore, $k_{t,ex} \approx k_{q,ex}$. The $k_{q,ex}$ increases with the extent of the double-bond conjugation of the CAR. Moreover, substituent groups at the end of the main polyene chain of the CAR play a role in $k_{q,ex}$. For example, both lycopene and β-carotene have a chromophore of nominally 11 conjugated double bonds, but lycopene achieves the larger $k_{q,ex}$ value, which is close to the diffusional limit in hexane (2.1×10^{10} M^{-1} s^{-1}). Steric hindrance between the polyene chain and the substituent end group results in changes in the effective conjugation of the double-bond system (36), altering the energy *E*(S) of the longest wavelength transition $\pi \rightarrow \pi^*(1^1A_g \rightarrow 1^1B_u)$ (36). In the case of β-carotene the steric effect induced by the β-rings at the end of the polyene chain produce a lack of effective conjugation and increases *E*(S).

Figure 5 shows the relationship between $\log(k_{q,ex})$ and *E*(S) in AOT reverse micelles at *W* = 5. The plot of $\log(k_{q,ex})$

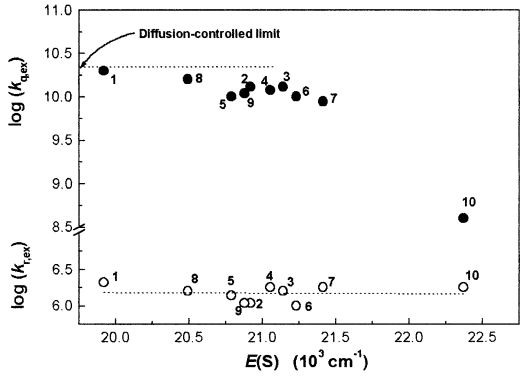

Figure 5. Empirical relationship between $\log(k_{q,ex})$ and $\log(k_{r,ex})$ with the energy E(S) of the longest wavelength transition $\pi \rightarrow \pi^*$ of the CAR in AOT–hexane–water ($W = 5$) reverse micelle solutions. Numbers label the CAR as shown in Table 3.

vs E(S) shows a functional dependence similar to that observed for other bimolecular deactivation processes in solution. A similar behavior has been shown for the $O_2(^1\Delta_g)$ quenching by a CAR series in chloroform homogeneous solutions (13).

According to Eq. 4 it is the triplet energy E(T) of the CAR that is decisive for the efficiency of the energy-transfer process. To our knowledge, there is a lack of information on the E(T) values of most CAR, except for β-carotene, the E(T) value of which has been determined as 88 kJ/mol (53). This value is comparable to the energy level of $O_2(^1\Delta_g)$ (94 kJ/mol). The exact relationship between the E(T) and E(S) is not known but can be assumed to be a proportionality of E(S) to E(T). Therefore, using the relationship between $\log(k_{q,ex})$ and E(S) (Fig. 5), it can be considered that for CAR with $E(S) > 21.0 \times 10^3$ cm^{-1} a thermal activation energy is required for quenching because the triplet energy of those CAR lies above the energy level of the donor $O_2(^1\Delta_g)$. At E(S) energies below 20.5×10^3 cm^{-1} the triplet energies become smaller than that of $O_2(^1\Delta_g)$, and additional thermal energy is no longer required for the quenching process, and the limit of $k_{q,ex}$ is given by the diffusion-controlled rate constant of the solvent.

For CAR without hydrogen-bonding donor substituent groups (*e.g.* lycopene, β-carotene, *etc.*) the $k_{q,ex}$ values were independent of W and similar to those observed in homogeneous hexane solutions (9). This result indicates that the CAR remain in the external pseudophase and that $[\Delta_{ex}]$ is constant, independent of the size and number of micellar aggregates present in the solution (29). In contrast, for CAR with hydrogen-bonding donor substituent groups, such as lutein, violaxanthin, bixin, small decreases in the $k_{q,ex}$ values with W were observed. As was discussed previously, these CAR are partially (*e.g.* lutein) or completely (*e.g.* bixin) associated with the AOT interface, respectively. In homogeneous media, the solvent polarity effect on the physical quenching rate constant of $O_2(^1\Delta_g)$ by CAR is rather complex (8–14,16,18); therefore, it is difficult to explain the observed quenching behavior by those CAR in reverse micelles by a polarity increment in the micellar interface as W increases. Probably, the decrease in $k_{q,ex}$ with W can be explained by a lower accessibility of $O_2(^1\Delta_g)$ to the reaction locus of the CAR at the micellar interface because the surfactant aggregation number increases with W (46).

Figure 5 also shows the relationship between $\log(k_{r,ex})$ and E(S) in AOT media. The reactive quenching rate constant $k_{r,ex}$ was found to be constant with E(S), *i.e.* independent of the extent of the double-bond conjugation (compare lycopene with 12′-apo-β-caroten-12′-oic acid).

In all cases, the reactive pathway involves a [4 + 2] or [2 + 2] cycloaddition reaction between the singlet ground state of the CAR and the electrophilic $O_2(^1\Delta_g)$ (54). Therefore, for large polyene systems, such as the CAR, the chemical attack of $O_2(^1\Delta_g)$ should be independent of the extent of the double-bond conjugation system.

It is interesting to note the solvent effect on the k_r value reported for bixin in homogeneous solutions, which in water was two orders of magnitude larger than that in dimethylsulphoxide (DMSO) and dimethylformamide (DMF) (16). The reactivity increment in a more polar solvent was explained in terms of an electron transfer process for the CAR bleaching. Our $k_{r,ex}$ values for bixin in AOT media were comparable to those reported in DMSO and DMF (16), in agreement with our assumption (see previously) that for the CAR bound to the AOT interface the double-bond–conjugated system is oriented to the organic pseudophase.

Photo-oxidation products: the β-carotene case

In all cases, upon prolonged illumination periods at the absorption band of RB, the disappearance of the original CAR absorption together with the appearance of new blueshifted absorption bands were observed (Fig. 4 for β-carotene). In this case, at illumination times longer than 16 min, the isosbestic point observed at *ca* 415 nm vanished, with the initiation of a spectral blueshift. This spectral behavior corresponds to the appearance of cleavage photo-oxidation products of β-carotene with a shorter double-bond conjugation system. Stratton *et al.* (54) have reported the photo-oxidation products of β-carotene on reaction with $O_2(^1\Delta_g)$ sensitized by RB in homogeneous toluene–methanol (85:15 vol/vol) solutions. The observed product pattern indicated that $O_2(^1\Delta_g)$ attacks at the 7,8-, 9,10-,11,12- or 13,14–double-bond positions, as expected for a long extended double-bond–conjugated system. The products of the reaction included chain cleavage products, such as β-apo-8′-carotenal, β-apo-10′-carotenal, β-apo-14′-carotenal and β-ionone, and a unique oxygen-addition product identified as β-carotene-5,8-endoperoxide (54). Product formation involving free radical (Type 1) reactions was ruled out because of the lack of production of 5,6- or 15,15′-epoxides, which are typical peroxyl radical oxidation products of β-carotene (54). Recently, Yamauchi *et al.* (55) confirmed the formation of β-carotene-5,8-endoperoxide and β-carotene-5,6-epoxide as oxidation products during the chlorophyll-sensitized photo-oxidation of methyl linoleate.

Our HPLC analysis of early-stage photolyzed solutions of β-carotene in AOT media indicated the formation of a single main product, with an elution time under our experimental conditions in agreement with that observed by Stratton *et al.* for β-carotene-5,8-endoperoxide (54). Furthermore, the UV–Vis absorption spectra of the product fraction obtained by

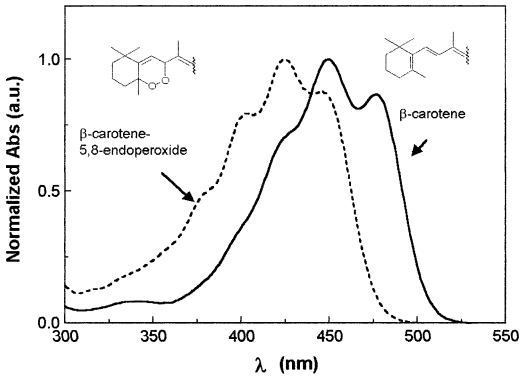

Figure 6. UV–Vis absorption spectra of β-carotene and of the primary photo-oxidation product β-carotene-5,8-endoperoxide formed by 1,4-cycloaddition of $O_2(^1\Delta_g)$ in AOT–hexane–water ($W = 5$) reverse micelle solutions.

preparative TLC (Fig. 6) was also in agreement with that reported previously (54).

After longer illumination periods of the solutions, using preparative TLC separation and HPLC analysis, we detected several shorter chain degradation products (which is probably the apo-CAR series), in agreement with the UV–Vis spectral behavior observed in Fig. 4.

Current research activities are being focused on the isolation and identification of $O_2(^1\Delta_g)$-mediated photo-oxidation products of other representative CAR, such as lycopene, lutein and bixine.

CONCLUSIONS

In summary, to our knowledge, the $O_2(^1\Delta_g)$ quenching (physical + chemical) by a CAR series in an AOT reverse micelle system has been studied for the first time. The $O_2(^1\Delta_g)$ generation was produced using the water-soluble anionic dye RB as the photosensitizer. The photophysical properties of RB indicated that the dye was located at the water–surfactant interface of the micellar aggregates. The UV–Vis properties of the CAR, such as the absorption maxima and the absorption band ratio %III/II, indicated that nonpolar CAR (carotenes) remain in the external pseudophase (hexane) of the micellar system. On the other hand, the spectral behavior for polar-CAR (xanthophylls) denoted that they interact with the micellar interface, with their double-bond–conjugated moiety oriented to the organic solvent.

Because of the compartmentalization of the sensitizer and the CAR in the micellar system, a pseudophase model was applied in order to obtain the respective physical ($k_{q,ex}$) and chemical ($k_{r,ex}$) quenching constants. It was assumed that the quenching process takes place in the external pseudophase (organic solvent + nonpolar interface). A good empirical relationship between $\log(k_{q,ex})$ and the energy $E(S)$ of the longest wavelength transition $\pi \rightarrow \pi^*$ of the CAR was found. The relationship showed that $k_{q,ex}$ converged to the diffusion-controlled limit value as $E(S)$ decreases. Because the $O_2(^1\Delta_g)$ physical quenching process depends on the energy of the triplet state $E(T)$ of the CAR, it can be extrapolated that CAR with $E(S) < 20.5 \times 10^3$ cm^{-1} are efficient quenchers of $O_2(^1\Delta_g)$.

On the other hand, the $k_{r,ex}$ was independent of the CAR and almost four orders of magnitude smaller than the $k_{q,ex}$. After prolonged photosensitization periods, the degradation of the CAR was observed with the formation of oxidation products with shorter polyene chain. In the case of β-carotene, the photo-oxidation at conversion values <10% yielded the 1,4-cycloaddition product β-carotene-5,8-endoperoxide as the main product. Current rsearch studies are being performed for the characterization of $O_2(^1\Delta_g)$-mediated photo-oxidation products of other representative CAR.

Acknowledgements—We thank the Consejo de Investigaciones Científicas y Técnicas (CICyT) de la Universidad Nacional de Santiago del Estero, the Consejo de Investigaciones Científicas y Tecnológicas de la Argentina (CONICET), Fundación Antorchas (Argentina) and the Agencia Nacional de Promocion Cientifica Tecnologicas (ANPCyT) for financial support and Prof. Peter Felker for help us in the manuscript preparation.

REFERENCES

1. Krinsky, N. I. (1989) Antioxidant functions of carotenoids. *Free Radic. Biol. Med.* **7**, 617–635.
2. Palozza, P. and N. I. Krinsky (1992) Antioxidant effects of carotenoids *in vivo* and *in vitro:* an overview. *Method Enzymol.* **213**, 403–420.
3. Spikes, J. D. (1989) Photosensitization. In *The Science of Photobiology,* 2nd ed. (Edited by K. C. Smith), pp. 79–110. Plenum Press, New York. [Chap. 3]
4. Wilkinson, F., W. P. Helman and A. B. Ross (1993) Quantum yields for the photosensitized formation of the lowest electronically excited singlet state of molecular oxygen in solution. *J. Phys. Chem. Ref. Data* **22**, 113–262.
5. Redmond, R. and J. N. Gamlin (1999) A compilation of singlet oxygen yields from biologically relevant molecules. *Photochem. Photobiol.* **70**, 391–475.
6. Foote, C. S. and R. W. Denny (1968) Chemistry of singlet oxygen. VII. Quenching by β-carotene. *J. Am. Chem. Soc.* **90**, 6233–6235.
7. Liebler, D. C. (1993) Antioxidant reactions of carotenoids. *Ann. N Y Acad. Sci.* **691**, 20–31.
8. Wilkinson, F. and J. G. Brummer (1981) Rate constants for the decay and reactions of the lowest electronically excited singlet state of molecular oxygen in solution. *J. Phys. Chem. Ref. Data* **10**, 809–999.
9. Conn, P., W. Schalch and T. G. Truscott (1991) The single oxygen and carotenoid interaction. *J. Photochem. Photobiol. B: Biol.* **11**, 41–47.
10. Oliveros, E., P. Murasecco-Suardi, A. M. Braun and H.-J. Hansen (1992) Efficiency of singlet oxygen quenching by carotenoids measured by near-infrared steady-state luminescence. *Methods Enzymol.* **213**, 420–429.
11. Di Mascio, P., A. R. Sundquist, T. P. A. Devasageyam and H. Sies (1992) Assay of lycopene and other carotenoids as singlet oxygen quenchers. *Methods Enzymol.* **213**, 429–438.
12. Hirayama, O., K. Nakamura, S. Hamada and Y. Kobayasi (1994) Singlet oxygen ability of naturally occurring carotenoids. *Lipids* **29**, 149–150.
13. Baltschun, D., S. Beutner, K. Briviba, H.-D. Martin, J. Paust, M. Peters, S. Röver, H. Sies, W. Stahl, A. Steigel and F. Stenhorst (1997) Singlet oxygen abilities of carotenoids. *Liebigs Ann.-Recl.* 1887–1893.
14. Edge, R., D. J. McGarvey and T. G. Truscott (1997) The carotenoids as anti-oxidants—a review. *J. Photochem. Photobiol. B: Biol.* **41**, 189–200.
15. Martin, H.-D., C. Jäger, C. Ruck, M. Schmidt, R. Walsh and J. Paust (1999) Anti- and prooxidant properties of carotenoids. *J. Prakt. Chem.* **341**, 302–308.
16. Speranza, G., P. Manitto and D. Monti (1990) Interaction between singlet oxygen and biologically active compounds in aqueous solutions. III. Physical and chemical $^1O_2$-quenching rate constants of 6,6′-diapocrotenoids. *J. Photochem. Photobiol. B: Biol.* **8**, 51–61.

17. Anderson, S. M. and N. I. Krinsky (1973) Protective action of carotenoid pigments against photodynamic damage to liposomes. *Photochem. Photobiol.* **18**, 403–408.
18. Fukuzawa, K. (2000) Singlet oxygen scavenging in phospholipid membranes. *Methods Enzymol.* **319**, 101–110.
19. Yin, M.-C. and W.-S. Cheng (1997) Oxymyoglobin and lipid oxidation in phospatidylcholine liposomes retarded by α-tocopherol and β-carotene. *J. Food Sci.* **62**, 1095–1097.
20. Fendler, H. (1982) *Membrane Mimetic Chemistry*. Wiley-Interscience, New York.
21. Kalyanasundaram, K. (1987) *Photochemistry in Microheterogeneous Systems.* Academic Press, Boca Raton, FL.
22. Lissi, E. A., M. V. Encinas, E. Lemp and M. A. Rubio (1993) Singlet oxygen $O_2(^1\Delta_g)$ bimolecular processes. Solvent and compartmentalization effects. *Chem. Rev.* **93**, 699–751.
23. Encinas, M. V. and E. A. Lissi (1986) Solubilization of neutral molecules in AOT inverse micelles in *n*-heptane. *Chem. Phys. Lett.* **132**, 545–548.
24. Miyoshi, N. and G. Tomita (1979) Quenching of singlet oxygen by sodium azide in reversed micelles systems. *Z. Naturforsch.* **34b**, 339–343.
25. Rodgers, M. A. J. and P. C. Lee (1984) Singlet molecular oxygen in micellar systems. 2. Quenching behavior in AOT reverse micelles. *J. Phys. Chem.* **88**, 3480–3484.
26. Liu, J., F. Zhang, Y. Zhao, F. Zhao, Y. Tang and X. Song (1997) Dye-sensitized photo-oxidation of amino acids in reversed micellar membrane mimetic system. *Sci. China Ser. B.* **40**, 84–91.
27. Biasutti, M. A., A. T. Soltermann and N. A. García (2000) Photodynamic effect in lysozyme: a kinetic study in different micellar media. *J. Peptide Res.* **55**, 41–50.
28. Milanesio, M. E., M. G. Alvarez, E. I. Yslas, C. D. Borsarelli, J. J. Silber, V. Rivarola and E. N. Durantini (2001) Photodynamic studies of metallo 5,10,15,20-tetrakis(4-methoxyphenyl) porphyrin: photochemical characterization and biological consequences in a human carcinoma cell line. *Photochem. Photobiol.* **74**, 14–21.
29. Rubio, M. A. and E. A. Lissi (1989) Photooxidation of anthracene derivatives in AOT/heptane reverse micelles. *J. Colloid Interface Sci.* **128**, 458–465.
30. Borsarelli, C. D., E. N. Durantini and N. A. García (1996) Singlet molecular oxygen-mediated photooxidation of nitrophenolic compounds in water-in-oil microemulsions. A kinetic study. *J. Chem. Soc. Perkin Trans.* **2**, 2009–2013.
31. Schiedt, K. and S. Liaaen-Jensens (1995) Isolation and analysis. In *Carotenoids Vol. 1a: Isolation and Analysis* (Edited by G. Britton, S. Liaaen-Jensens and H. Pfander), pp. 81–108. Birkhäuser Verlag, Basel.
32. Mercadante, A. Z., D. B. Rodriguez-Amaya (1990) Carotenoid composition and vitamin A value of some native Brazilian green leafy vegetables. *Int. J. Food Sci. Technol.* **25**, 213–219.
33. Arima, H. K. and D. B. Rodriguez-Amaya (1988) Carotenoids composition and vitamin A value of commercial Brazilian squashes and pumpkins. *J. Micronutr. Anal.* **4**, 177–191.
34. Rodriguez-Amaya, D. B. and C. A. Tavares (1992) Importance of *cis*-isomer separation in determining provitamin A in tomato and tomato products. *Food Chem.* **45**, 297–302.
35. Mercadante, A. Z. (1999) Chromatographic separation of carotenoids. *Arch. Latinoam. Nutr.* **49**, 52–57.
36. Britton, G. (1995) UV/visible spectroscopy. In *Carotenoids Vol. 1B: Spectroscopy* (Edited by G. Britton, S. Liaaen-Jensens and H. Pfander), pp. 13–63. Birkhäuser Verlag, Basel.
37. Cardoso, S. L., D. E. Nicodem, T. A. Moore, A. L. Moore and D. Gust (1996) Synthesis and fluorescence quenching studies of a series of carotenoporphyrins with carotenoids of various length. *J. Braz. Chem. Soc.* **7**, 19–30.
38. Correa, N. M., E. N. Durantini and J. J. Silber (2001) Substituent effects on binding constant of carotenoids to *n*-heptane/AOT reverse micelles. *J. Colloid Interface Sci.* **240**, 573–580.
39. Neckers, D. C. (1989) Rose Bengal. *J. Photochem. Photobiol. A: Chem.* **47**, 1–29.
40. Rodgers, M. A. J. (1984) Picosecond studies of rose bengal fluorescence in reverse micellar systems. In *Reverse Micelles* (Edited by P. L. Luisi and B. E. Straub), pp. 165–173. Plenum Press, New York.
41. Zinsli, P. E. (1979) Inhomogeneous interior of aerosol OT microemulsions probed by fluorescence and polarization decay. *J. Phys. Chem.* **83**, 3223–3231.
42. Borsarelli, C. D., J. J. Cosa and C. M. Previtali (1992) Exciplex formation between pyrene derivatives and *N,N′*-dimethylaniline in aerosol OT reverse micelles. *Langmuir* **8**, 1070–1075.
43. Borsarelli, C. D. and S. E. Braslavsky (1997) Nature of the water structure inside the pools of reverse micelles sensed by laser-induced optoacoustic spectroscopy. *J. Phys. Chem. B* **101**, 6036–6042.
44. Green, F. (1991) *The Sigma–Aldrich Handbook of Stains, Dyes and Indicators*, 2nd ed. Aldrich Chemical Company, Milwaukee.
45. Jeffrey, S. W., R. F. C. Mantoura and S. W. Wright (1997) Phytoplankton Pigments in Oceanography: Guidelines to Modern Methods. Unesco publishing, Paris.
46. Lang, J., A. Jada and A. Malliaris (1988) Structure and dynamics of water-in-oil droplets stabilized by sodium bis(2-ethylhexyl)sulfosuccinate. *J. Phys. Chem.* **92**, 1946–1953.
47. Lee, P. C. and M. A. J. Rodgers (1983) Singlet molecular oxygen in micellar systems. 1. Distribution equilibria between hydrophobic and hydrophilic compartments. *J. Phys. Chem.* **87**, 4894–4898.
48. Turro, N. J., M. Aikawa and A. Yekta (1979) Dynamics of molecular oxygen in micellar solutions. *Chem. Phys. Lett.* **64**, 473–478.
49. Martínez, L. A., C. G. Martínez, B. B. Klopotek, J. Lang, A. Neuner, A. M. Braun and E. Oliveros (2000) Nonradiative and radiative deactivation of singlet molecular oxygen ($O_2(^1\Delta_g)$) in micellar media and microemulsions. *J. Photochem. Photobiol. B: Biol.* **58**, 94–107.
50. Nonell, S. (1994) Reactive oxygen species. In *Photobiology in Medicine* (Edited by G. Jori), pp. 29–50. Plenum Press, New York.
51. Redmond, R. (1991) Enhancement of the sensitivity of radiative and non-radiative detection techniques in the study of photosensitization by water soluble sensitizers using a reverse micelle system. *Photochem. Photobiol.* **54**, 547–556.
52. Lambert, C. R. and I. E. Kochevar (1996) Does rose bengal triplet generate superoxide anion? *J. Am. Chem. Soc.* **118**, 3297–3298.
53. Haley, J. L., A. N. Fitch, R. Goyal, C. Lambert and T. G. Truscott (1992) The S_1 and T_1 energy levels of all-trans -β-carotene. *J. Chem. Soc. Chem. Commun.* **17**, 1175–1176.
54. Stratton, S. P., W. H. Schaeffer and D. C. Liebler (1993) Isolation and identification of singlet oxygen oxidation products of β-carotene. *Chem. Res. Toxicol.* **6**, 542–547.
55. Yamauchi, R., K. Tsuchihashi and K. Kato (1998) Oxidation products of β-carotene during the peroxidation of methyl linoleate in the bulk phase. *Biosci. Biotechnol. Biochem.* **62**, 1301–1306.